Nonlinear Dyn (2025) 113:7243–7258
https://doi.org/10.1007/s11071-024-10729-1

RESEARCH

Synchronization levels in EEG connectivity during cognitive workloads while driving

Nafise Naseri · Fatemeh Parastesh · Farnaz Ghassemi · Sajad Jafari · Matjaž Perc · Jernej Završnik

Received: 29 September 2024 / Accepted: 26 November 2024 / Published online: 11 December 2024

Abstract Understanding the impact of cognitive workload on neuronal synchronization and brain network structure is crucial for deciphering brain function across various cognitive tasks. This study explores how different levels of cognitive workload influence brain activity during driving, focusing on urban and motorway settings with and without traffic. By analyzing the phase locking value of EEG data from 20 drivers, we identify distinct changes in brain functional connectivity patterns, in high versus low cognitive workloads, particularly in the delta and theta bands. Scenarios with higher cognitive workload reveal a less efficient network structure and decreased small-worldness, especially within the delta and theta bands during urban driving. Frontal and occipital-parietal nodes show a greater tendency to cluster in low cognitive workload conditions compared to high workload, particularly in low-frequency EEG bands. These results provide significant insights into the neural mechanisms of cognitive load, with implications for enhancing cognitive task design and developing future real-time applications in fields like driving assistance and workload management.

Keywords Complex networks · Synchronization · EEG · Cognitive workload · Driving

N. Naseri · F. Ghassemi · S. Jafari
Department of Biomedical Engineering, Amirkabir University of Technology (Tehran Polytechnic), Tehran, Iran

F. Parastesh
Center for Research, SRM Easwari Engineering College, Chennai, India

F. Parastesh
Center for Research, SRM Institute of Science and Technology, Chennai, India

S. Jafari
Health Technology Research Institute, Amirkabir University of Technology (Tehran Polytechnic), Tehran, Iran

M. Perc
Faculty of Natural Sciences and Mathematics, University of Maribor, Koroška cesta 160, 2000 Maribor, Slovenia

M. Perc · J. Završnik
Community Healthcare Center Dr. Adolf Drolc Maribor, Vošnjakova ulica 2, 2000 Maribor, Slovenia

M. Perc
Complexity Science Hub Vienna, Josefstädterstraße39, 1080 Vienna, Austria

M. Perc (✉)
Department of Physics, Kyung Hee University, 26 Kyungheedae-ro, Dongdaemun-gu, Seoul, Republic of Korea
e-mail: matjaz.perc@gmail.com

1 Introduction

The study of neuroscience requires a thorough understanding of the brain's operations during various tasks [1]. This can be done by analyzing the results of mathematical neural models or the recorded electrical activity of the brain. While computational models and numerical simulations provide theoretical insights into brain network dynamics [2–4], examining neurobiological

signals that directly represent brain activity offers a more robust empirical grasp of brain function [5].

Neuroscientists are interested in the brain's response to cognitive or physical engagements [6]. This entails thoroughly analyzing how various cognitive and physical tasks affect brain activity and subsequent responses [7]. In this investigation, the term *"workload"* is crucial, as it refers to the amount of mental or physical effort needed to complete a task [8]. Examining the workload associated with different tasks can help scientists discover the brain's functioning and adaptation to different demands [9,10].

The amount of effort that is required to perform mental tasks is referred to as the cognitive workload [11]. The cognitive workload is strongly tied to allocating resources to working memory and its relationship with attentional processes [12]. The variability in cognitive workload across contexts offers valuable opportunities for elucidating the neural mechanisms that underpin cognitive processing and task performance. Driving, in particular, presents a fascinating domain for such research due to its multifaceted cognitive requirements [13]. Planning, making decisions, and paying attention to visual cues are examples of high-level mental processes that are needed for driving, although it is a low-level physical action [14,15]. To ensure safe driving, each of these duties needs to be completed promptly and precisely. As a result, driving requires a high level of concentration, skill, and experience.

When driving, cognitive workload is quite important [15]. Numerous factors, including traffic conditions, navigational tasks, and distractions inside the car, can impact it. A high cognitive workload may reduce driving ability and raise the chance of accidents. For example, a study discovered that one of the main contributing factors to traffic crashes is complicated traffic situations and a high driving workload [16]. Another study explored the impact of distracting activities in a city scenario on driving workload and performance [17]. The findings demonstrated that driving workload and performance are affected when engaging in a secondary task. These studies show that changes in the individual or environmental factors that affect a driver's performance behind the wheel can lead to fluctuations in the workload of that driver.

Analyzing the network formed by neurons' interactions provides a deeper comprehension of the brain's cognitive workload levels. Although functional magnetic resonance imaging (fMRI) is often regarded as the gold standard for recording neuronal activity due to its superior spatial resolution, the high temporal resolution of electroencephalogram (EEG) signals is particularly well-suited for capturing rapid neural changes, such as those occurring during fast-paced tasks like driving. EEG functional connectivity, which measures the statistical interdependence of different EEG channels, can be used to map the network of neuronal interactions [18]. This enables a comprehensive understanding of the brain's network dynamics by giving connectivity adjacency matrices. Once these networks have been formed, complex network theory can be applied to further examine them. This theoretical framework enables the investigation of emergent phenomena in the brain's network, such as chimera states [19–21] and synchronization patterns [22–24], even in higher-order networks [25]. In essence, integrating complex network theory with EEG functional connectivity offers a thorough method for illustrating the collective actions of the brain, illuminating its complex dynamics and functionality.

In recent years, studies have examined the network's local and global characteristics to investigate cognitive load. Kaposzta et al. found that a higher mental workload was associated with a decrease in large-scale functional connections during n-back working memory paradigm [26]. Similarly, Dimitrakopoulos et al. discovered that when workload rose, brain networks, as estimated by the Phase Locking Index (PLI), showed a statistically significant drop in both the clustering coefficient and small-worldness metrics [27]. Furthermore, Xu et al. suggested that dynamic features might be useful indicators of mental workload levels [28]. These findings highlight the intricate relationship between brain network properties and cognitive workload. Notably, most prior studies have investigated brain network analysis across various cognitive workload levels during tasks like n-back working memory or numerical calculations. However, there is limited understanding of how functional brain connectivity networks operate at different cognitive load levels during driving tasks. This motivates us to examine the global and local properties of the brain network across various cognitive load levels during driving.

The purpose of this research is to investigate how different levels of cognitive workload affect brain activity dynamics during driving by utilizing EEG functional connectivity and graph theory. We hypothesize that variations in cognitive workload will impact neu-

ronal synchronization in EEG frequency bands, particularly in regions related to attention and cognitive control, such as the frontal cortex, with observable changes between low and high cognitive load conditions. The study compares brain functional networks under high and low cognitive workloads, which are associated with driving in high-traffic and low-traffic conditions within a driving simulation, respectively. The impact of different cognitive workload levels is analyzed separately for two specific driving environments: urban and motorway roads. The key contributions of this paper are as follows: (1) Unlike previous studies that explored tasks unrelated to driving, this study addresses the effects of cognitive workload on brain connectivity in driving scenarios. (2) EEG functional connectivity is evaluated through the Phase Locking Value (PLV) across various frequency bands to understand how neural synchrony changes with cognitive workload levels during driving tasks. (3) Functional brain networks are analyzed using graph theory, comparing both local and global network characteristics, such as path length, node strength, clustering coefficient, efficiency, and transitivity, across two cognitive workload levels. (4) A comprehensive analysis of connectivity patterns across different brain regions is conducted, revealing how cognitive workload affects interactions between the frontal, occipital, and parietal areas.

Five sections make up the remainder of the paper. Section 2 describes the EEG data and the graph-based algorithms. Subsequently, Sections 3 and 4 show the results and discussion that were achieved. Section 5 concludes with some findings.

2 Materials and method

2.1 Experimental data

This study utilizes a public EEG dataset comprising 20 male participants with an age range of 22 to 42 and valid driving licenses [29]. Driving tasks were performed in a driving simulation with automatic transmission mode, using standard paths and minimal path changes to decrease task-related physical activity. The experimental sessions were conducted in a quiet environment with constant lighting and air conditioning to minimize distractions like head movements or eye blinks. These sessions took place mainly in the morning, and participants were advised to get plenty of sleep and were not allowed to talk to anyone else during the sessions. EEG recordings were conducted at a sampling rate of 256 Hz with 24 electrodes following the international 10−20 system, referencing the Cz electrode. Figure 1 displays the names and positions of these electrodes.

The EEG data was recorded in driving simulation conditions. The protocol comprised a practice session aimed at acquainting participants with the driving simulator and simulation software. The subsequent four sessions involved driving scenarios in motorway (M-scenario) and urban (U-scenario) routs:

1. Motorway without cars: Participants drove on a motorway without the presence of other cars.
2. Motorway with cars: Participants traversed the motorway with the addition of AI-controlled cars, leading to a 70% vehicle traffic density (70% of the road's space is occupied by vehicles).

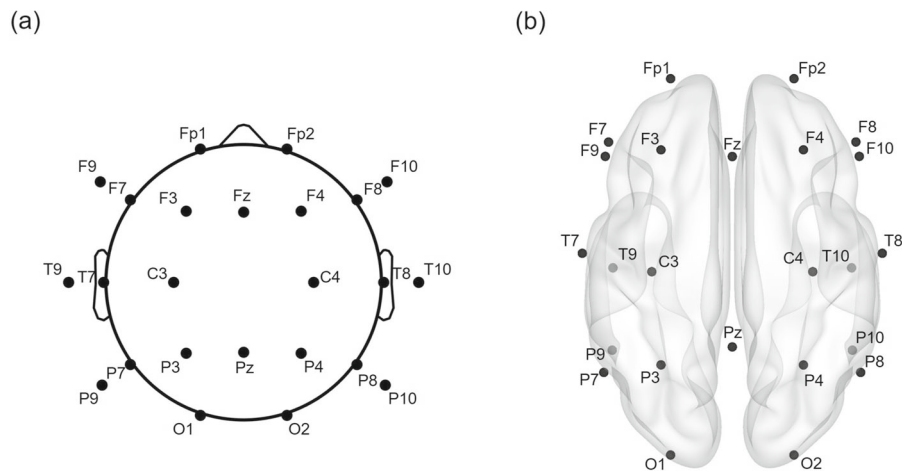

Fig. 1 Electrode positioning for EEG data collection under the international 10−20 system. The placement of all 24 electrodes utilized for recording EEG data in this study, presented in **a** 2D and **b** 3D views. The Cz electrode is employed as the reference for the setup

3. Urban without cars: Participants drove in an urban area without the presence of other cars.
4. Urban with cars: Participants traversed the urban area with the addition of AI-controlled cars, leading to a 30% vehicle traffic density (30% of the road's space is occupied by vehicles).

Each session lasted seven to 10 min, with a five-minute break between them to reduce fatigue. Participants rated the workload for four driving tasks on a scale of one to ten, where one represented the lowest workload and ten the highest. The comparisons emphasize that tasks involving interactions with other cars induce a substantially higher workload than scenarios without such interactions. The mean ratings for M-scenarios with and without cars were 3.7 (High Cognitive Workload, HCW) and 1.85 (Low Cognitive Workload, LCW), respectively, with a significant difference between them (P-value $= 0.001$, ANOVA test). Also, the mean ratings for U-scenarios with cars (4.9, HCW) and without cars (2.65, LCW) differed significantly (P-value $= 0.0005$, ANOVA test) [29].

2.2 EEG pre-processing

All data preprocessing steps were performed using the EEGLAB toolbox in MATLAB [30]. Initially, a bandpass Finite Impulse Response (FIR) filter with a cutoff frequency ranging from 1 to 40 Hz was applied to the EEG data using the `eegfiltnew` function. Subsequently, channels exhibiting flat activity for more than five seconds, indicative of non-functioning electrodes, were determined and removed using the FlatlineCriterion option within the `clean_rawdata` function. The Artefact Subspace Reconstruction (ASR) was employed for the identification and correction of high-variance artifacts associated with motor activity like blink artifacts [31]. This was performed using the `clean_rawdata` function with a BurstCriterion parameter set to 20 and a LineNoiseCriterion parameter set to 4. Any missing channels were then effectively interpolated using spherical interpolation (`interp` function), with only minimal reconstruction required (1 channel in 16 conditions and 2 channels in 2 conditions across all participants and conditions). This method leverages data from surrounding electrodes to estimate missing signals. Furthermore, the common average reference (CAR) was used to mitigate uncorrelated noise using the `reref` function [32]. This technique involves referencing each channel to the average signal of all channels. Ultimately, the signals were epoched into non-overlapping eight-second segments. The number of segments obtained per participant varied according to the specific experimental condition and duration of each recording session.

2.3 Functional connectivity network

To evaluate the phase synchronization of two EEG signals, the Phase Locking Value (PLV) can be used. This metric reveals the rate of phase synchronization of two signals, separate from their amplitude. Taking ϕ_1 and ϕ_2 as the phase of two oscillators, and their relative as $\Delta\phi = |\phi_1 - \phi_2|$, PLV can be defined as:

$$PLV = |\langle \exp(j\Delta\phi_{rel}) \rangle|, \tag{1}$$

in which, $\langle . \rangle$ denotes the time average, j is the imaginary unit, and $\Delta\phi_{rel} = \Delta\phi \bmod 2\pi$ [33]. If two signals are phased-locked, the PLV would be equal to one. Otherwise, they have a lower positive PLV. Despite some volume conduction effect vulnerabilities, PLV is a useful tool for understanding connectivity dynamics of cognitive load during driving tasks because of its sensitivity to phase synchronization and real-time applicability. Furthermore, as the total number of channels utilized in this analysis is relevantly low, PLV of this data results in a reduced volumetric conduction effect. In this paper, the PLV has been calculated for all EEG bands, including delta (δ, 1 to 4 Hz), theta (θ, 4 to 8 Hz), alpha (α, 8 to 13 Hz), beta (β, 13 to 30 Hz) and gamma (γ, 30 to 40 Hz). The phases were estimated using the Hilbert transform. Since low-weighted connections may provide important insights into workload-induced connectivity changes, unthresholded adjacency matrices are kept to maintain both high- and low-weighted connections.

2.4 Connectivity graph analysis

The connectivity matrices can be analyzed using graph theory and complex network analysis. Graph-based metrics can be used to evaluate graph features, including integration and segregation. Integration and segregation provide key concepts for understanding how information flows within these networks. A network's

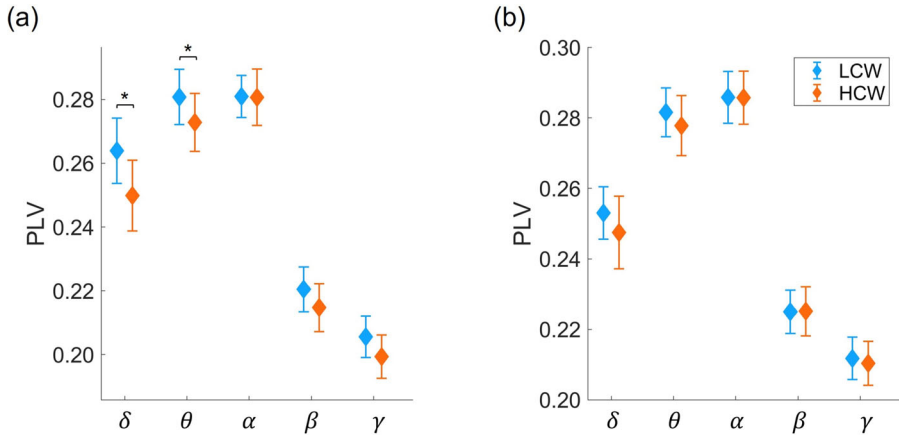

Fig. 2 The error bars for the mean Phase Locking Value (PLV) of the drivers in **a** the urban (U-scenario) and **b** the motorway (M-scenario) environments across EEG frequency bands. Blue lines indicate Low Cognitive Workload (LCW), and orange lines indicate High Cognitive Workload (HCW). In the U-scenario, significant decreases in synchronization are observed for HCW compared to LCW in the delta (P-value $= 0.006$) and theta (P-value $= 0.027$) bands, as denoted by stars, suggesting lower connectivity during high workload. Conversely, the M-scenario shows no significant PLV differences across EEG bands between workload levels. These results imply that cognitive workload has a more pronounced effect on neural synchronization in urban driving conditions than in motorway conditions

integration refers to how well its components are connected, facilitating information transmission. Segregation, however, identifies separate clusters or communities inside the network, indicating specialized information processing or compartmentalization. Graph-based indexes such as the clustering coefficient capture the degree of local clustering or community structure, which reflects a network's segregation. Meanwhile, measurements like average shortest path length and global efficiency provide insight into the network's integration capability by quantifying how effectively information is distributed throughout it. While clustering coefficient and efficiency capture overlapping information in networks with less than 50 nodes, examining both metrics yields complementary insights: clustering coefficient shows interconnectivity of nodes' neighbors, whereas efficiency focuses on overall network communication.

Different aspects of the network's topology can be captured using these metrics, which may exhibit local or global characteristics. Local characteristics capture the network's immediate environment by concentrating on single nodes or tiny groups of nodes. Global features, on the other hand, provide a more comprehensive view and describe the general topology of the network. Analyzing both local and global features of graph-based metrics can help gain insights into the dynamics and function of complex networks, which helps comprehend how integration-segregation balance within them.

In this paper, for all the weighted adjacency matrices of PLV in each band, three local (node strength (k), local clustering coefficient (CC_L), and local efficiency (E_L)) and four global (characteristic path length (PL), global clustering coefficient (CC_G), global efficiency (E_G), and transitivity (Tr)) graph-based features are calculated. Definitions, formulas, and additional details for these metrics can be found in the Appendix.

3 Results

Various synchronization levels are determined by calculating the mean PLV of each group's workload level. The sign rank Wilcoxon test with an alpha level of 0.05 is used to decide whether there is a significant difference between HCW and LCW in each EEG band, as the Kolmogorov-Smirnov (KS) normality test is rejected. Figure 2 displays the mean PLV error bar for each EEG band under both scenarios, with LCW displayed in blue and HCW in orange. In the U-scenario (Fig. 2a), the HCW PLV is significantly lower than the LCW in the delta (LCW 0.258 ± 0.039; HCW 0.249 ± 0.047; P-

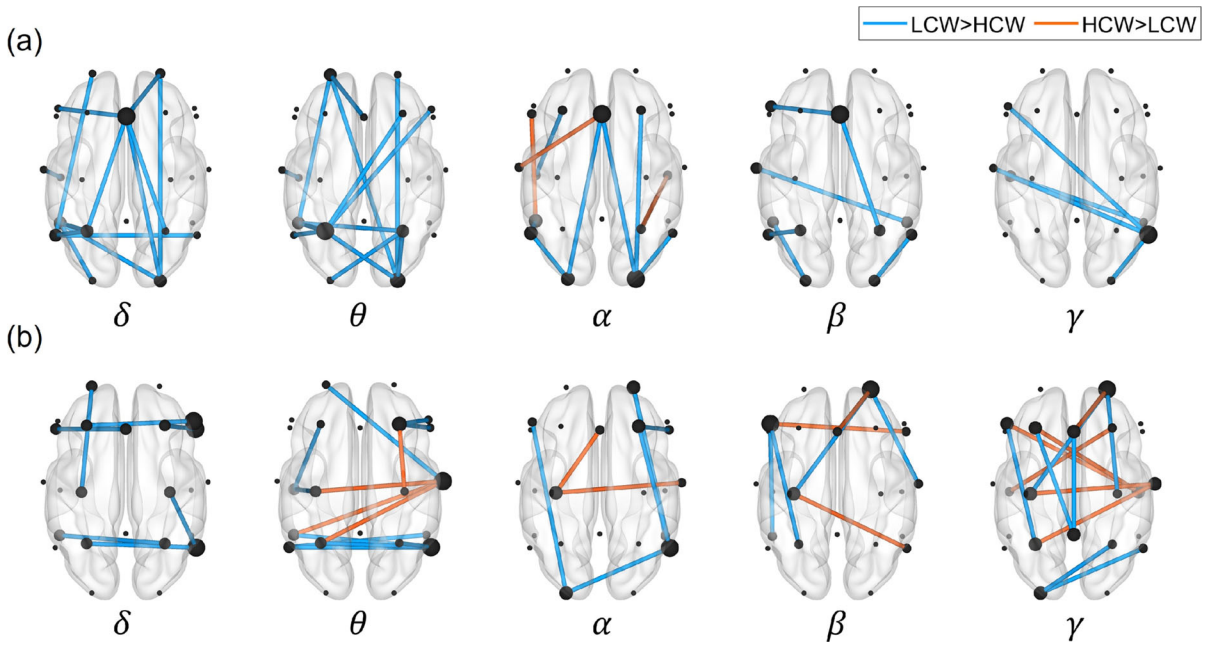

Fig. 3 Channel-by-channel PLV connections of driver brain functional networks in the **a** urban (U-scenario) and **b** motorway (M-scenario) settings across EEG frequency bands, using a one-tailed Wilcoxon test (alpha level of 0.01) to identify significant differences between Low Cognitive Workload (LCW) and High Cognitive Workload (HCW). Blue links represent connections with significantly higher PLV in LCW than HCW, while orange links indicate higher PLV in HCW. The larger nodes are the ones with more connected links. In the U-scenario, LCW exhibits significantly stronger connectivity in the delta and theta bands compared to HCW, particularly around the Fz and P3 channels, indicating more widespread connectivity. In the M-scenario, differences in overall mean PLV between LCW and HCW are less pronounced, although LCW shows stronger inter-hemispheric connectivity in the delta and theta bands. These results indicate that cognitive workload level affects connectivity patterns more distinctly in the U-scenario than in the M-scenario

value = 0.006) and theta bands (LCW 0.281 ± 0.035; HCW 0.275 ± 0.039; *P*-value = 0.027); while in the M-scenario (Fig. 2b), there is no significant variation between EEG bands at the two levels.

To gain further insight, each channel's PLV connection is analyzed in Fig. 3. The figure illustrates the obtained result of a one-tailed Wilcoxon test with an alpha level of 0.01 on each EEG channel connection. Given the risk of Type I errors arising from multiple pairwise comparisons, a stricter alpha level of 0.01 was applied to minimize false positives. The blue links show the connectivity of those in LCW with significantly higher PLV than those in HCW, whereas the orange link indicates the greater connectivity of those in HCW than LCW. In the U-scenario (Fig. 3a), the LCW connections are typically stronger than the HCW ones. In the delta band, no node's connection in HCW is stronger than in LCW. A blue network in which LCW has a larger PLV than HCW exhibits several strong anterior-posterior connections. In addition, in this network, the Fz channel has more connectivity to the right and left hemispheres than other channels. In the theta band, only the blue network is visible, indicating that no node's PLV is stronger in HCW than in LCW. This band mostly shows inter-hemispheric connections, with the P3 channel serving as the hub for the majority of the inter-hemispheric connections. It means that the connectivity that alters between the two cognitive workload levels in this band is primarily inter-hemispheric. In the other three bands, there is not much variance in the connection between cognitive workload levels. Some intra-hemispheric connections are found to be stronger in HCW than in LCW in the alpha band. In this band, a few anterior-posterior connections have also been seen, which are mostly the ones that are stronger in LCW than HCW. Blue connectivity is identified in the beta band with a small number of intra- and inter-hemispheric connections (mostly Fz connections) and also in the

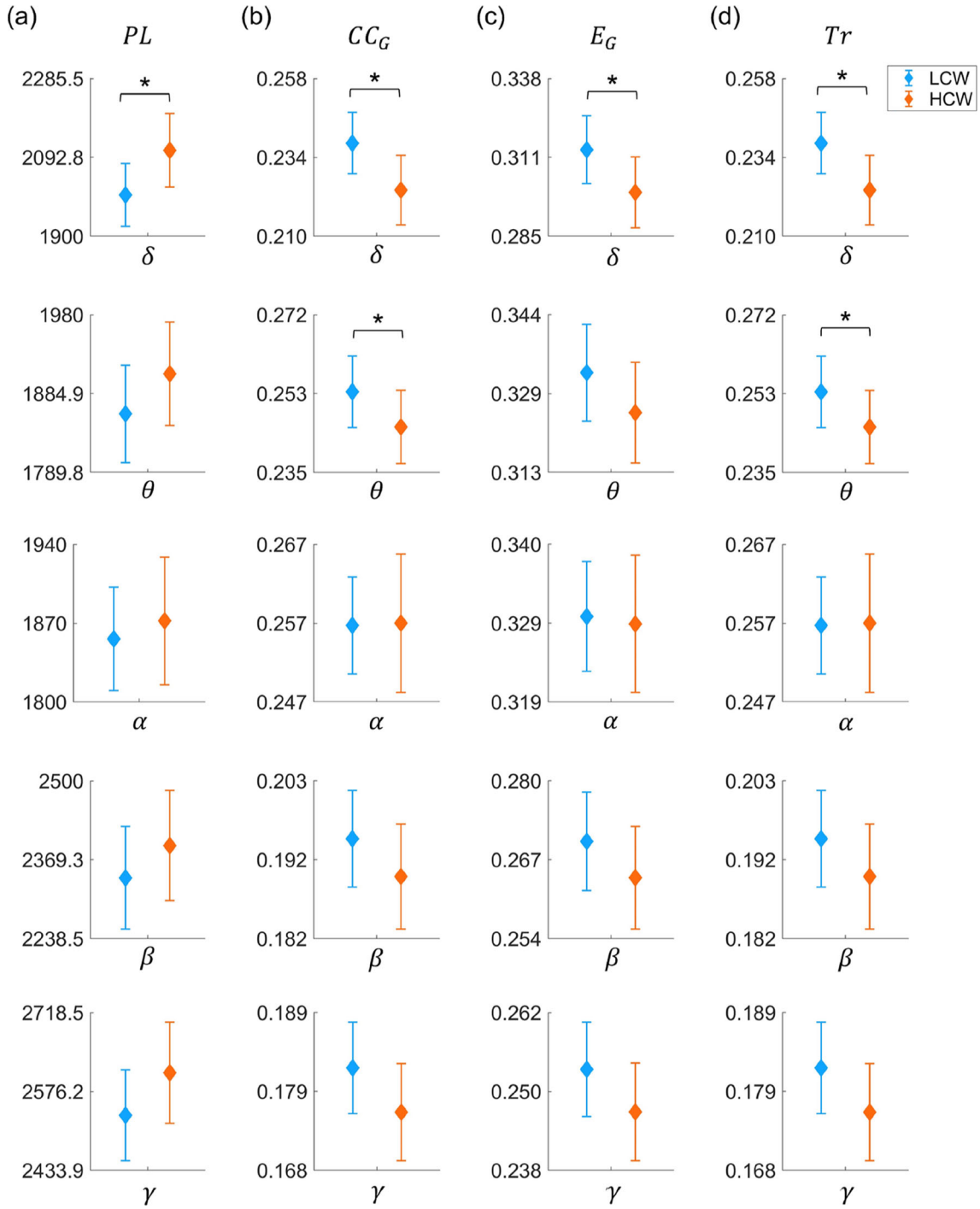

Fig. 4 Global graph-based features of PLV connectivity matrices in Low Cognitive Workload (LCW) and High Cognitive Workload (HCW) conditions in the urban (U-scenario) environment. Error bars for **a** characteristic path length (PL), **b** global clustering coefficient (CC_G), **c** global efficiency (E_G), and **d** transitivity (Tr) illustrate significant differences between LCW and HCW in the delta and theta bands, with a significance threshold of P-value < 0.05 (indicated by stars). HCW shows a notable reduction in CC_G (P-value $= 0.002$) and increased PL (P-value $= 0.027$) in the delta band, implying a decrease in network integration and a longer path for information flow under high cognitive demand. Similarly, lower E_G (P-value $= 0.015$) and Tr (P-value $= 0.002$) in HCW suggest reduced parallel processing capacity and weaker network clustering, respectively, indicative of a more decentralized network in the delta and theta bands. These results highlight that higher cognitive workload disrupts small-world properties and information processing efficiency in the U-scenario

gamma band with few inter-hemispheric connections (mainly P8 connections).

Figure 3b exhibits the connectivity in the M-scenario, which indicates a significant distinction between LCW and HCW in each band. However, the mean PLV differs significantly between the two cognitive workload levels in no band. In the delta band, HCW has no stronger connections than LCW. The blue network contains some inter-hemispheric connections in the frontal and parietal lobes. In the theta band, some inter-hemispheric connections in the parietal and central lobes can be seen in blue (stronger LCW) and orange (stronger HCW) connections, respectively. Both the blue and orange networks exhibit some intra- and inter-hemispheric connections in the alpha and beta bands. In the gamma band, inter-hemispheric connections are particularly prominent in the orange network of the central to parietal and frontal lobes.

Through graph analysis, the network of the mean PLV is investigated further. For all EEG bands of LCW and HCW in both scenarios, four global graph-based features (PL, CC_G, E_G, and Tr) are computed. Due to the non-normality of the data, the difference between each group has been examined using a Wilcoxon test with an alpha level of 0.05. Since the HCW condition in the U-scenario has a lower CC (LCW 0.238 ± 0.041; HCW 0.224 ± 0.047; P-value $= 0.002$) and a longer PL (LCW 2000.9 ± 343.1; HCW 2110.0 ± 400.7; P-value $= 0.027$) than the LCW condition shown in Fig. 4, it exhibits less small-worldness in the delta band. Its global efficiency (LCW 0.314 ± 0.050; HCW 0.300 ± 0.053; P-value $= 0.015$) and transitivity (LCW 0.238 ± 0.041; HCW 0.224 ± 0.047; P-value $= 0.002$) are also lower. Moreover, HCW in the theta band has a lower global clustering coefficient (LCW 0.254 ± 0.037; HCW 0.245 ± 0.038; P-value $= 0.018$) and transitivity (LCW 0.254 ± 0.037; HCW 0.246 ± 0.038; P-value $= 0.018$). Reduced global efficiency in HCW reveals slower parallel information processing and the lowest cognitive function in delta and theta bands, and lower transitivity reveals weaker clustering, indicating a decentralized network topology in delta and theta bands. As Fig. 5 illustrates, there is no significant difference in the global feature between HCW and LCW in the M-scenario.

Additionally, for every node in each EEG band of LCW and HCW, three local graph-based features are extracted: k, CC_L, and E_L. The local characteristics of the U- and M-scenarios are displayed in Figs. 6 and 7, respectively. Every EEG band shows a common pattern for each local feature. The central electrodes exhibit the lowest features. The anterior and posterior electrodes have the highest features in the low-frequency bands, whereas the anterior values are lower in the high-frequency bands.

In addition to this pattern, the Wilcoxon test has been used to statistically compare the local features between two cognitive workload levels. Channels with significant variations in local features between low and high cognitive workloads (P-value < 0.05) are bolded. It has been observed that for all three local features in the U-scenario, the frontal and occipital-parietal nodes differ mostly in the delta and theta bands. The frontal and occipital nodes in these two bands display greater local features in LCW than in HCW. There are not many nodes that differ significantly in these features across the alpha, beta, and gamma bands. Only a few posterior channels are bolded as distinct channels. The left channels in the beta band and the right ones in the gamma band have shown the majority of these differences.

The M-scenario exhibits the same pattern of low local features in the central channels at low frequencies and high local features in the anterior and posterior channels as the U-scenario. Also, the anterior value drops in high-frequency bands. The nodes with varying values of local features can seldom be observed in other bands; however, no significant variation in features between workload levels has been observed in the delta and beta bands.

4 Discussion

This paper examines the EEG functional connectivity of men driving on motorway (M-scenario) and urban (U-scenario) roads with varying workload levels using complex network and graph analysis. This investigation may help in understanding how different cognitive workloads affect brain synchronization. Calculating PLV connectivity and graph-based features in each EEG band reveals the variation in brain synchrony between high and low cognitive workloads. It was observed that the mean PLV in the M-scenario does not differ across workload levels. However, in the U-scenario, delta and theta bands exhibit significantly higher PLV in LCW than in HCW. In all bands of the U- and M-scenarios, LCW has higher occipital-parietal region connectivity, particularly in the delta and theta

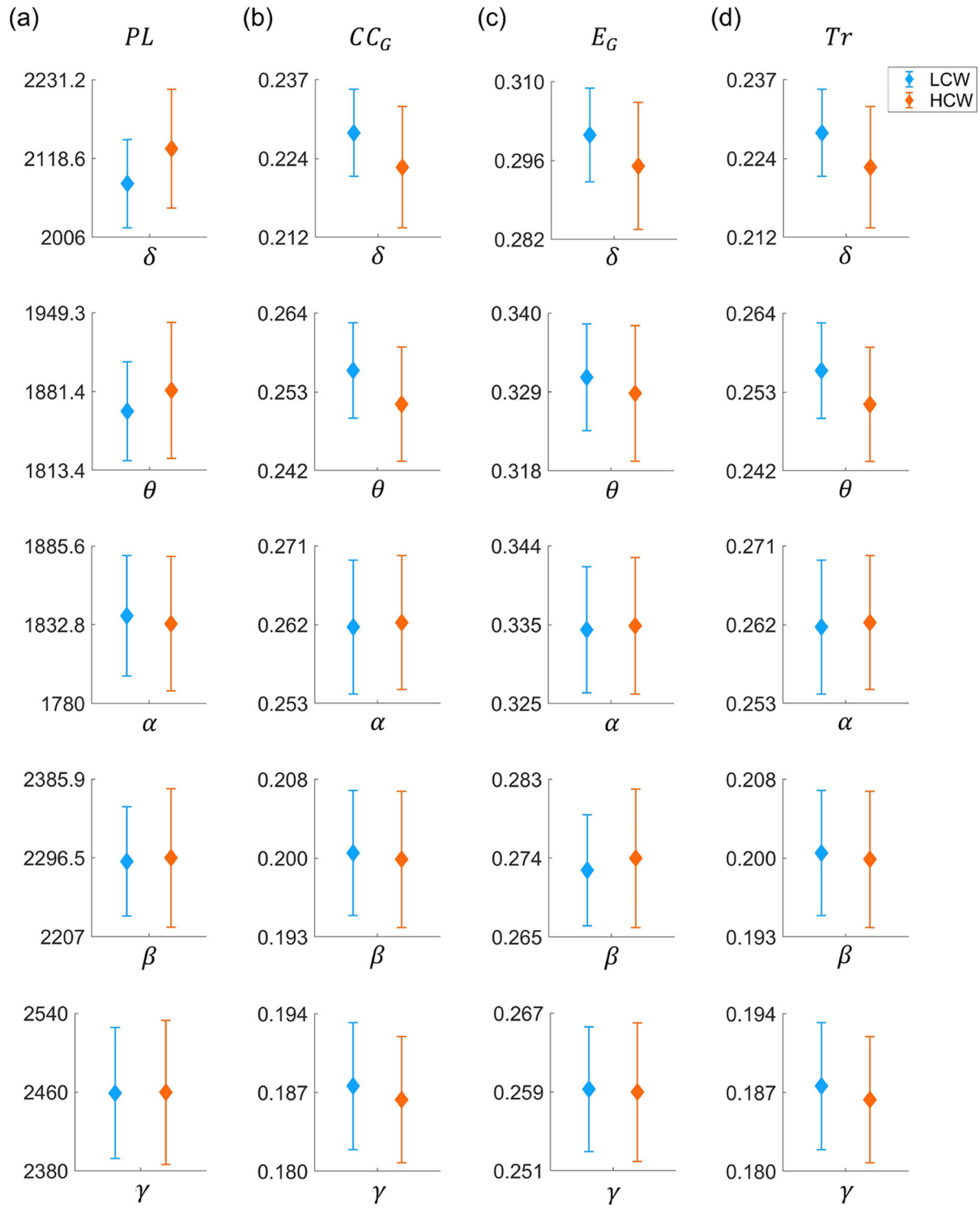

Fig. 5 Global graph-based features of PLV connectivity matrices in Low Cognitive Workload (LCW) and High Cognitive Workload (HCW) conditions in the motorway (M-scenario) environment. Error bars for **a** characteristic path length (PL), **b** global clustering coefficient (CC_G), **c** global efficiency (E_G), and **d)** transitivity (Tr) reveal no statistically significant differences between LCW and HCW across EEG bands (P-value < 0.05). This finding suggests that, unlike the urban setting, cognitive workload level in the M-scenario does not substantially affect these global connectivity features

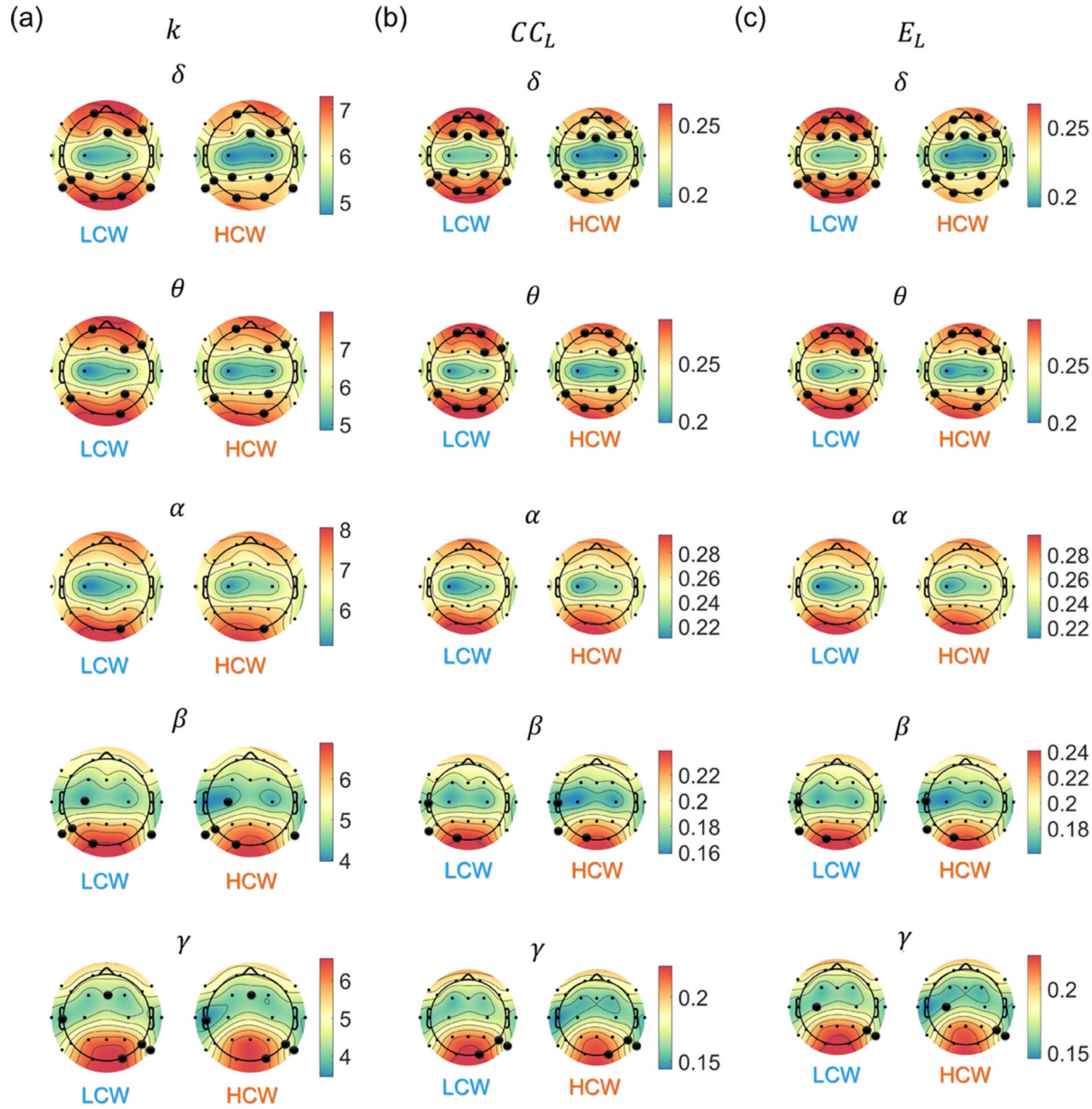

Fig. 6 Topographical distribution of local graph-based features in Low Cognitive Workload (LCW) and High Cognitive Workload (HCW) for the urban (U-scenario) environment across EEG frequency bands. The topo plots illustrate the spatial distribution of **a** Node strength (k), **b** local clustering coefficient (CC_L), and **c** local efficiency (E_L) for each workload level. Warmer colors indicate higher feature values. Local features are highest in the anterior and posterior electrodes for low-frequency bands and decrease in the high-frequency bands. Central electrodes exhibit consistently low feature values across all bands. Notable differences between LCW and HCW appear primarily in the delta and theta bands, where frontal and occipital-parietal nodes display significantly higher local features in LCW (P-value < 0.05), as indicated by bolded channels. These findings suggest that cognitive workload influences localized connectivity patterns in the U-scenario, with LCW associated with stronger local network integration in frontal and occipital regions, particularly in the lower frequency bands

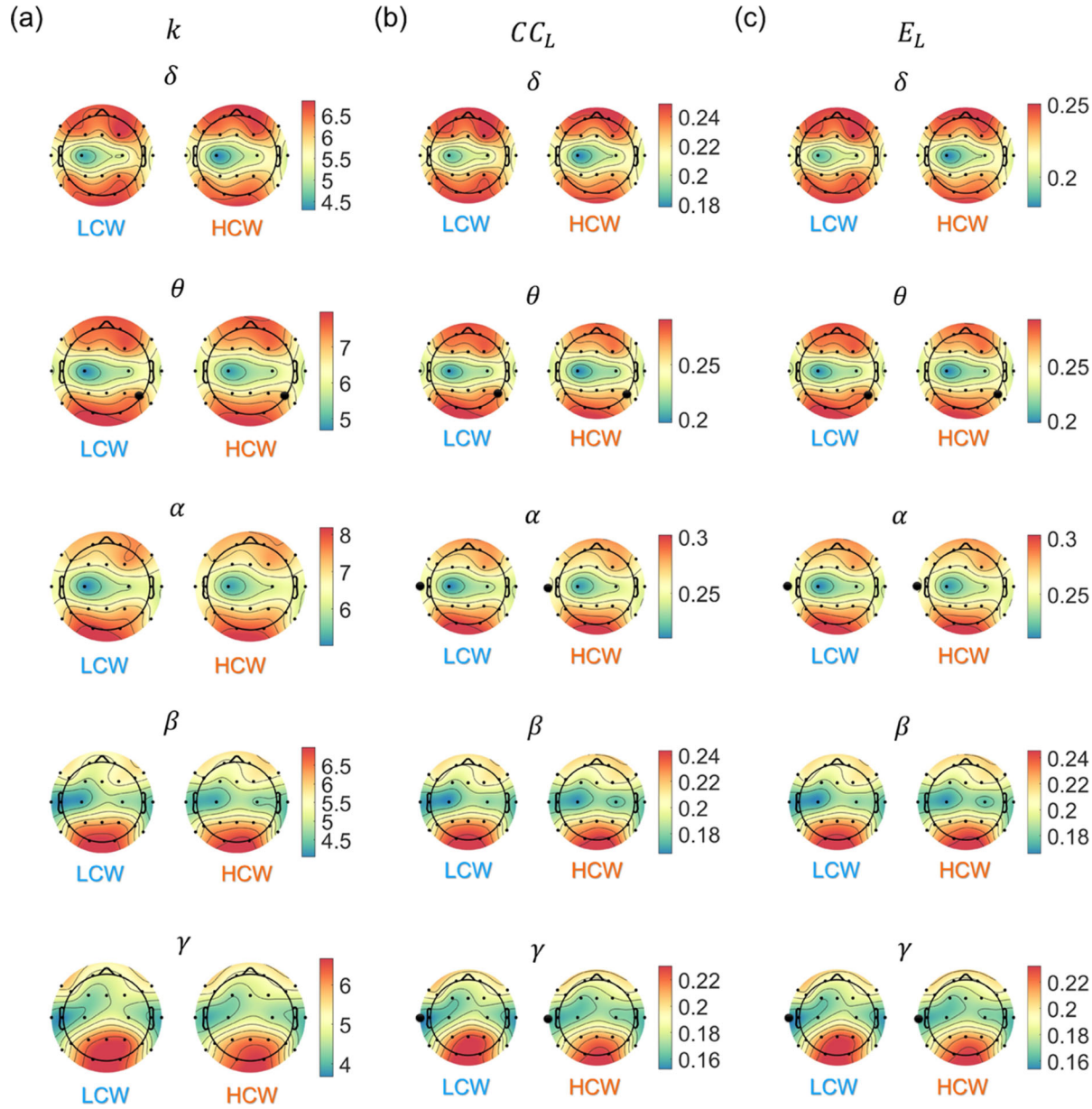

Fig. 7 Topographical distribution of local graph-based features in Low Cognitive Workload (LCW) and High Cognitive Workload (HCW) for the motorway (M-scenario) environment across EEG frequency bands. The topo plots depict the spatial distribution of **a** Node strength (k), **b** local clustering coefficient (CC_L), and **c** local efficiency (E_L) for LCW and HCW conditions. Warmer colors represent higher feature values. Central regions show lower feature values, while anterior and posterior regions exhibit higher local features at lower frequencies. The high-frequency bands demonstrate a decrease in anterior features. Differences between LCW and HCW are limited, with only a few notable variations in other bands

bands. According to Dimitrakopoulos et al. [34], frontal theta activity, is a reliable indicator of cognitive task difficulty. Frontal theta activity was found to be strongly correlated with mental workload [35]. It has also been demonstrated that the PLV of theta and alpha bands in the frontal and occipital-parietal brains reflects cognitive load [36]. Figure 3 showed that in the theta band in the U-scenario, occipital-parietal PLV connectivity is higher in LCW than in HCW, while in the M-scenario, frontal and occipital PLV connectivity is higher. In addition, both scenarios show higher occipital-parietal PLV in the alpha band. Given that the frontal cortex is crucial for executive control, attention, and cognitive regulation, while the occipital-parietal regions are essential for processing visual information and managing spatial attention, these findings highlight how these brain areas work together to handle cognitive demands. Specifically, this pattern suggests that the connections within the frontal and occipital-parietal regions are particularly efficient, especially during tasks such as driving, which require sustained attention and sensorimotor integration. Other studies have found strong functional connectivity in the fronto-centro-temporo-parietal regions for the theta band during a dual task with a high mental workload [37]. Higher theta EEG power spectrums were observed in individuals driving army ground vehicles under the most difficult workload conditions [38].

Research has indicated that when driving, as compared to rest, the power of delta waves, theta, and frontal theta asymmetry increases, which has been attributed to the cognitive load that driving environments impose [39]. It has also been discovered that the delta-alpha and delta-theta ratios substantially correlate with various driving states, including city-roadways driving state and expressway driving state. This discovery offers insights into the neural reactions to differing cognitive workloads during driving. In our study, under U-scenarios, the delta band had the highest functional connectivity in LCW, almost across all brain regions. Furthermore, in the M-scenario, some frontal and occipital high connectivity was observed in LCW in this band.

Using graph metrics, we demonstrated that different workload levels in the U-scenario differ in the delta and theta bands, whereas there were no significant differences in the M-scenario. Also, the U-scenario's HCW has a lower global clustering coefficient and a higher characteristic path length, indicating a lower small-worldness in the delta band. The study [40] indicated that the clustering coefficient is useful in determining cognitive load from EEG signals. Higher workloads were also observed during mental arithmetic and n-back tasks, resulting in lower clustering coefficients and small-worldness metrics [27]. Ref. [41] demonstrated that a higher workload correlates with lower clustering values. Furthermore, our finding showed that in the U-scenario, LCW exhibits higher CC and Tr in the delta and theta bands compared to HCW. A high transitivity in LCW indicates that nodes tend to have more clusters, resulting in densely connected subgraphs of the network. Nodes in these networks may have fewer random connections or form more cohesive clusters. Other computed features with their corresponding results are defined below:

- Local clustering coefficient: A local clustering coefficient can be used to describe the topology of the regional network and to identify regions of the network that exhibit strong clustering tendencies. In the U-scenario, the LCW shows higher local CC in the frontal and occipital-parietal regions in the delta and theta bands than the HCW. This finding further emphasizes the role of the frontal and occipital-parietal regions in tasks with varying cognitive demands that require effective communication and integration.
- Global efficiency: The ability of a network to transfer information between every pair of nodes is measured by its global efficiency. In the U-scenario, LCW has higher global efficiency and a lower path length in the delta band. A higher global efficiency indicates that there are shorter paths between nodes in the network, allowing for more effective communication.
- Local efficiency: The resilience of local communication inside the network is measured by local efficiency. In the U-scenario, compared to HCW, the LCW shows higher local efficiency in frontal and occipital-parietal regions in the delta and theta bands. High local efficiency highlights the robustness of local connections by showing that the network can maintain efficient communication even when specific nodes are removed, highlighting the resilience of local connectivity.
- Node strength: Nodes with high strength are essential to network connection and performance because they have a greater impact on information flow and overall network performance. Network node

strength analysis can identify important nodes that act as hubs or crucial points for communication and influence. These nodes, which enable effective information transfer and coordination among various network components, are frequently essential to the structure and dynamics of the network. It was found that the frontal and occipital node strengths in the delta and theta bands are higher in LCW than in HCW.

5 Conclusion

Human performance and efficiency are intimately related to cognitive workload in various circumstances, particularly when driving a car. In this paper, the EEGs of 20 male drivers were analyzed to determine how their cognitive workload levels varied in different situations. The obtained functional connectivity matrices were investigated using complex network and graph theories on two motorway and urban routes defined as the M- and U-scenarios, respectively. In the M-scenario, there was no difference in Phase Locking Value (PLV) values or global graph-based features between low cognitive workloads (LCW) and high cognitive workloads (HCW), with only a few channels having different local features between the two groups. Meanwhile, in the U-scenario's delta band, LCW has a shorter path length (PL) but a higher clustering coefficient (CC), efficiency (E), and transitivity (Tr) than HCW. In the theta band, this group has a higher CC and Tr than HCW. Both of these bands had higher PLV values in LCW compared to HCW. It revealed that safe driving requires effective management of the cognitive workload. When there are other vehicles on the road in an urban environment, it is critical for drivers to devote sufficient attention to the road to prevent their cognitive load from getting too high. Moreover, the results suggest potential applications for assistive technologies in semi-autonomous vehicles, which could use real-time EEG-based connectivity measures to detect cognitive overload and activate supportive features for safer driving. This can lower the chance of an accident and enhance driving performance.

Future research should investigate the sensitivity and specificity of these connectivity measures in comparison to other neurophysiological indices, such as frontal theta power, to refine workload detection systems. Notably, all the results were derived from male drivers, making it inapplicable to generalize the findings to female drivers. It would be valuable to conduct a similar study on female drivers and compare the gender differences in cognitive workload under various driving scenarios. Additionally, the use of a driving simulation environment may limit the applicability of the findings to real-world conditions. Thus, future studies should validate these results in more realistic settings to enhance their practical relevance.

Funding M.P. was supported by the Slovenian Research and Innovation Agency (Javna agencija za znanstvenoraziskovalno in inovacijsko dejavnost Republike Slovenije) (Grant Nos. P1-0403).

Data Availability The data that support the findings of this study are openly available at https://figshare.com/articles/dataset/Data_Characterisation_of_Cognitive_Load_using_Machine_Learning_Classifiers_of_Electroencephalogram_Data/23978112. (https://doi.org/10.17862/cranfield.rd.23978112)

Declarations

Conflict of interest The authors declare that they have no Conflict of interest.

Appendix

The following definitions and formulas detail each of the graph-based metrics.

1. Node strength: Node strength (k) is used to quantify the importance or influence of individual nodes in a network. It considers both the weights attached to a node's connections and the total number of connections (its degree). A node's strength, which is determined by adding up the weights of all the edges that are incident to it, indicates how well the node can communicate with other nodes in the network. Taking $w_{i,\ell}$ to be the weighted linkages between nodes i and ℓ, and N as the set of all nodes in the network, the strength of node i can be calculated as:

$$k_i = \sum_{\ell \in N} w_{i,\ell}.$$

2. Clustering coefficient: The clustering coefficient (CC) is a quantitative indicator of how tightly nodes cluster together in a network. The local clustering coefficient counts the fraction of a node's neighbors who are also connected to one another. The local

CC for node i can be defined as follows [42]:

$$CC_L(i) = \frac{2t_i}{k_i(k_i-1)}.$$

In this equation, t_i represents the weighted geometric mean of triangles around node i, namely:

$$t_i = \frac{1}{2}\sum_{\substack{\ell,h\in N\\ i\neq\ell\neq h}} \left(w_{i,\ell}\, w_{i,h}\, w_{\ell,h}\right)^{\frac{1}{3}}.$$

For $k_i < 2$, $CC_L(i) = 0$. By averaging the local CC of every node in the network, global CC is obtained. This metric measures the overall tendency of nodes in the network to form cohesive clusters or triangles. Considering n as the number of nodes, global CC is computed as follows:

$$CC_G = \frac{1}{n}\sum_{i\in N} CC_L(i).$$

3. Characteristic path length: Characteristic path length (PL), also known as average path length, is a global measure of network connectedness that takes the average of the shortest path lengths between all node pairs in the network. It is useful for describing a network's connectivity and navigation features. A weighted network's PL can be defined as [43]:

$$PL = \frac{1}{n}\sum_{i\in N}\frac{\sum_{\ell\in N,\ \ell\neq i} d_{i,\ell}}{n-1},$$

in which $d_{i,\ell}$ is the weighed shortest path length between nodes i and ℓ.

4. Efficiency: Efficiency (E) provides insights into how effectively information is transmitted between networks. This measure is crucial for evaluating the overall connectedness and integration of the network, particularly in complex brain networks. Local efficiency explores how effectively information may be moved in the immediate neighborhood of a node when that node is removed. It is defined as the average inverse shortest path length between a node's neighbors [44]:

$$E_L(i) = \frac{\sum_{\ell\in N,\ \ell\neq i} d_{i,\ell}^{-1}}{n-1}.$$

On the other hand, the average inverse shortest path length between all pairs of nodes is used to determine global efficiency:

$$E_G = \frac{1}{n}\sum_{i\in N} E_L(i).$$

5. Transitivity: Transitivity (Tr) is a fundamental notion that quantifies the tendency of nodes in a network to create closed loops or triangles of connections. It can be defined mathematically as the ratio of connected triples of nodes to triangles in the network [45]:

$$Tr = \frac{\sum_{i\in N} 2t_i}{\sum_{i\in N} k_i(k_i-1)}.$$

References

1. Bassett, D.S., Sporns, O.: Network neuroscience. Nat. Neurosci. **20**(3), 353–364 (2017)
2. Yang, Y., Ma, J., Xu, Y., Jia, Y.: Energy dependence on discharge mode of Izhikevich neuron driven by external stimulus under electromagnetic induction. Cognit. Neurodyn. **15**, 265–277 (2021)
3. Xu, Q., Liu, T., Ding, S., Bao, H., Li, Z., Chen, B.: Extreme multistability and phase synchronization in a heterogeneous bi-neuron Rulkov network with memristive electromagnetic induction. Cognit. Neurodyn. **17**(3), 755–766 (2023)
4. Ding, S., Wang, N., Bao, H., Chen, B., Wu, H., Xu, Q.: Memristor synapse-coupled piecewise-linear simplified Hopfield neural network: dynamics analysis and circuit implementation. Chaos Solitons Fractals **166**, 112899 (2023)
5. Timmermann, C., Roseman, L., Haridas, S., Rosas, F.E., Luan, L., Kettner, H., Martell, J., Erritzoe, D., Tagliazucchi, E., Pallavicini, C., Girn, M., Alamia, A., Leech, R., Nutt, D.J., Carhart-Harris, R.L.: Human brain effects of DMT assessed via EEG-fMRI. Proc. Natl. Acad. Sci. **120**(13), 2218949120 (2023)
6. Strömmer, J.M., Põldver, N., Waselius, T., Kirjavainen, V., Järveläinen, S., Björksten, S., Tarkka, I.M., Astikainen, P.: Automatic auditory and somatosensory brain responses in relation to cognitive abilities and physical fitness in older adults. Sci. Rep. **7**(1), 13699 (2017)
7. Degirmenci, M., Yuce, Y.K., Perc, M., Isler, Y.: EEG-based finger movement classification with intrinsic time-scale decomposition. Front. Hum. Neurosci. **18**, 1362135 (2024)
8. Bernhardt, K.A., Poltavski, D., Petros, T., Ferraro, F.R., Jorgenson, T., Carlson, C., Drechsel, P., Iseminger, C.: The effects of dynamic workload and experience on commercially available EEG cognitive state metrics in a high-fidelity air traffic control environment. Appl. Ergonom. **77**, 83–91 (2019)
9. Zhou, Y., Xu, Z., Niu, Y., Wang, P., Wen, X., Wu, X., Zhang, D.: Cross-task cognitive workload recognition based on EEG and domain adaptation. IEEE Trans. Neural Syst. Rehabil. Eng. **30**, 50–60 (2022)
10. Dehais, F., Lafont, A., Roy, R., Fairclough, S.: A neuroergonomics approach to mental workload, engagement and human performance. Front. Neurosci. **14**, 519228 (2020)
11. Paas, F., Renkl, A., Sweller, J.: Cognitive load theory and instructional design: Recent developments. Educ. Psychol. **38**(1), 1–4 (2003)

12. Jaquess, K.J., Gentili, R.J., Lo, L.-C., Oh, H., Zhang, J., Rietschel, J.C., Miller, M.W., Tan, Y.Y., Hatfield, B.D.: Empirical evidence for the relationship between cognitive workload and attentional reserve. Int. J. Psychophysiol. **121**, 46–55 (2017)
13. Broadbent, D.P., D'Innocenzo, G., Ellmers, T.J., Parsler, J., Szameitat, A.J., Bishop, D.T.: Cognitive load, working memory capacity and driving performance: a preliminary fNIRS and eye tracking study. Transp. Res. Part F Traffic. Psychol. Behav. **92**, 121–132 (2023)
14. Kircher, K., Ahlstrom, C.: Minimum required attention: a human-centered approach to driver inattention. Hum. Factors **59**(3), 471–484 (2017)
15. Recarte, M.A., Nunes, L.M.: Mental workload while driving: effects on visual search, discrimination, and decision making. J. Exp. Psychol. **9**(2), 119 (2003)
16. Lyu, N., Xie, L., Wu, C., Fu, Q., Deng, C.: Driver's cognitive workload and driving performance under traffic sign information exposure in complex environments: A case study of the highways in China. Int. J. Environ. Res. Public Health **14**(2), 203 (2017)
17. Luo, S., Yi, X., Shao, Y., Xu, J.: Effects of distracting behaviors on driving workload and driving performance in a city scenario. Int. J. Environ. Res. Public Health **19**(22), 15191 (2022)
18. Cao, J., Zhao, Y., Shan, X., Wei, H.-L., Guo, Y., Chen, L., Erkoyuncu, J.A., Sarrigiannis, P.G.: Brain functional and effective connectivity based on electroencephalography recordings: a review. Hum. Brain Mapp. **43**(2), 860–879 (2022)
19. Majhi, S., Bera, B.K., Ghosh, D., Perc, M.: Chimera states in neuronal networks: a review. Phys. Life Rev. **28**, 100–121 (2019)
20. Li, X., Xie, Y., Ye, Z., Huang, W., Yang, L., Zhan, X., Jia, Y.: Chimera-like state in the bistable excitatory-inhibitory cortical neuronal network. Chaos Solitons Fractals **180**, 114549 (2024)
21. Xu, Y., Lu, L., Ge, M., Jia, Y.: Effects of temporally correlated noise on coherence resonance chimeras in FitzHugh-Nagumo neurons. Eur. Phys. J. B **92**, 1–10 (2019)
22. Yan, B., Parastesh, F., He, S., Rajagopal, K., Jafari, S., Perc, M.: Interlayer and intralayer synchronization in multiplex fractional-order neuronal networks. Fractals **30**(10), 2240194 (2022)
23. Chen, X., Wang, N., Wang, K., Chen, M., Parastesh, F., Xu, Q.: Coupling dynamics in an FHN bi-neuron model coupled via ReLU function-based locally active memristor. Nonlinear Dyn. **112**, 20365–20379 (2024)
24. Yao, Z., Wang, C., Zhou, P., Ma, J.: Regulating synchronous patterns in neurons and networks via field coupling. Commun. Nonlinear Sci. Numer. Simul. **95**, 105583 (2021)
25. Parastesh, F., Mehrabbeik, M., Rajagopal, K., Jafari, S., Perc, M.: Synchronization in Hindmarsh-Rose neurons subject to higher-order interactions. Chaos **32**(1), 013125 (2022)
26. Kaposzta, Z., Stylianou, O., Mukli, P., Eke, A., Racz, F.S.: Decreased connection density and modularity of functional brain networks during n-back working memory paradigm. Brain Behav. **11**(1), 01932 (2021)
27. Dimitrakopoulos, G.N., Kakkos, I., Anastasiou, A., Bezerianos, A., Sun, Y., Matsopoulos, G.K.: Cognitive reorganization due to mental workload: a functional connectivity analysis based on working memory paradigms. Appl. Sci. **13**(4), 2129 (2023)
28. Xu, Z., Huang, J., Liu, C., Zhang, Q., Gu, H., Li, X., Di, Z., Li, Z.: Dynamic functional connectivity correlates of mental workload. Cognitive Neurodynamics **18**(5), 2471–2486 (2024). https://doi.org/10.1007/s11571-024-10101-4
29. Wang, Q., Smythe, D., Cao, J., Hu, Z., Proctor, K.J., Owens, A.P., Zhao, Y.: Characterisation of cognitive load using machine learning classifiers of electroencephalogram data. Sensors **23**(20), 8528 (2023)
30. Delorme, A., Makeig, S.: EEGLAB: An open source toolbox for analysis of single-trial EEG dynamics including independent component analysis. J. Neurosci. Methods **134**(1), 9–21 (2004)
31. Mullen, T.R., Kothe, C.A., Chi, Y.M., Ojeda, A., Kerth, T., Makeig, S., Jung, T.-P., Cauwenberghs, G.: Real-time neuroimaging and cognitive monitoring using wearable dry EEG. IEEE Trans. Biomed. Eng. **62**(11), 2553–2567 (2015)
32. Ludwig, K.A., Miriani, R.M., Langhals, N.B., Joseph, M.D., Anderson, D.J., Kipke, D.R.: Using a common average reference to improve cortical neuron recordings from microelectrode arrays. J. Neurophysiol. **101**(3), 1679–1689 (2009)
33. Lachaux, J.-P., Rodriguez, E., Martinerie, J., Varela, F.J.: Measuring phase synchrony in brain signals. Hum. Brain Mapp. **8**(4), 194–208 (1999)
34. Dimitrakopoulos, G.N., Kakkos, I., Dai, Z., Lim, J., deSouza, J.J., Bezerianos, A., Sun, Y.: Task-independent mental workload classification based upon common multiband EEG cortical connectivity. IEEE Trans. Neural Syst. Rehabil. Eng. **25**(11), 1940–1949 (2017)
35. Hamann, A., Carstengerdes, N.: Investigating mental workload-induced changes in cortical oxygenation and frontal theta activity during simulated flights. Sci. Rep. **12**(1), 6449 (2022)
36. Dimitriadis, S.I., Sun, Y., Kwok, K., Laskaris, N.A., Thakor, N., Bezerianos, A.: Cognitive workload assessment based on the tensorial treatment of EEG estimates of cross-frequency phase interactions. Ann. Biomed. Eng. **43**, 977–989 (2015)
37. Shaw, E.P., Rietschel, J.C., Shuggi, I.M., Xu, Y., Chen, S., Miller, M.W., Hatfield, B.D., Gentili, R.J.: Cerebral cortical networking for mental workload assessment under various demands during dual-task walking. Exp. Brain Res. **237**, 2279–2295 (2019)
38. Diaz-Piedra, C., Sebastián, M.V., Di Stasi, L.L.: EEG theta power activity reflects workload among army combat drivers: an experimental study. Brain Sci. **10**(4), 199 (2020)
39. Hussain, I., Young, S., Park, S.-J.: Driving-induced neurological biomarkers in an advanced driver-assistance system. Sensors **21**(21), 6985 (2021)
40. Zhu, G., Zong, F., Zhang, H., Wei, B., Liu, F.: Cognitive load during multitasking can be accurately assessed based on single channel electroencephalography using graph methods. IEEE Access **9**, 33102–33109 (2021)

41. Sciaraffa, N., Borghini, G., Aricò, P., Di Flumeri, G., Colosimo, A., Bezerianos, A., Thakor, N.V., Babiloni, F.: Brain interaction during cooperation: evaluating local properties of multiple-brain network. Brain Sci. **7**(7), 90 (2017)
42. Onnela, J.-P., Saramäki, J., Kertész, J., Kaski, K.: Intensity and coherence of motifs in weighted complex networks. Phys. Rev. E **71**(6), 065103 (2005)
43. Li, X., Jing, Z., Hu, B., Zhu, J., Zhong, N., Li, M., Ding, Z., Yang, J., Zhang, L., Feng, L.: A resting-state brain functional network study in MDD based on minimum spanning tree analysis and the hierarchical clustering. Complexity **2017**(1), 9514369 (2017)
44. Latora, V., Marchiori, M.: Efficient behavior of small-world networks. Phys. Rev. Lett. **87**(19), 198701 (2001)
45. Rubinov, M., Sporns, O.: Complex network measures of brain connectivity: uses and interpretations. Neuroimage **52**(3), 1059–1069 (2010)